Adsorption (2007) 13: 509–514
DOI 10.1007/s10450-007-9055-z

Pore characterization of assembly-structure controlled single wall carbon nanotube

M. Arai · M. Kanamaru · T. Matsumura · Y. Hattori · S. Utsumi · T. Ohba · H. Tanaka · C.M. Yang · H. Kanoh · F. Okino · H. Touhara · K. Kaneko

Received: 11 June 2007 / Revised: 10 September 2007 / Accepted: 13 September 2007 / Published online: 3 October 2007

Abstract Single wall carbon nanotube (SWCNT), which has bundle structure and entangled structure, was untangled and cut by sonication in hydrogen peroxide (H_2O_2) solution. The untangled state of SWCNT was examined by SEM, TEM, Raman spectroscopy and N_2 adsorption. It was confirmed that the surface area of sonicated nanotubes strongly depended on the sonication time. The BET specific surface area (SSA) of nanotubes sonicated for 3 h was maximum. The SSA decreased at 6 h or more of sonication time. These results indicated that the bundle structure was untangled and the cap of SWCNT was opened. Thus, N_2 molecules can access the most efficiently inside of the SWCNT sonicated for 3 h. On the contrary, the sonication treatment for 6 h or more decomposed the nanotubes to produce amorphous carbon, evidenced by TEM and SEM observation; the amorphous carbon blocked the open pore sites such as the internal pore spaces and interstitial pores.

Keywords Carbon nanotube · Nanopore characterization · Micropore filling · Raman spectroscopy · Molecular simulation

Abbreviations

ΔE	The change of energy in the system
T	Temperature (K)
$\Phi(r)$	Lennard-Jones potential energy
r	The distance between the center of particle i and particle j (Å)
ε_{ij}	The particle i-particle j potential well depth
σ_{ij}	The effective distance between the center of particle i and particle j (Å)
k_B	Boltzmann constant (J/K)
P/P_0	Relative pressure

M. Arai · M. Kanamaru · T. Matsumura · Y. Hattori · S. Utsumi · T. Ohba · H. Tanaka · C.M. Yang · H. Kanoh · K. Kaneko (✉)
Graduate School of Science, Chiba University, 1-33 Yayoi, Inage, Chiba 263-8533, Japan
e-mail: kaneko@pchem2.s.chiba-u.ac.jp

F. Okino · H. Touhara
Faculty of Textile Science and Technology, Shinshu University, 3-15-1 Tokida, Ueda 386-8567, Japan

1 Introduction

Single wall carbon nanotube (SWCNT) has gathered great attention in various fields of science and technology (Saito et al. 2000). Ordinary SWCNTs have *bundle structures* which are also entangled with each other (Hirsch 2002), although Hata et al. succeeded to prepare highly pure SWCNTs which are mutually isolated (Hata et al. 2004). The bundle structure provides interstitial nanopores of the very strong interaction potential for molecules and thereby the designated bundle structure is preferable for the application of SWCNT as an adsorbent, membrane filter, and gas sensor (Cao et al. 2003). If the geometry of the SWCNT bundle, such as the tubule length, bundle thickness and intertube distance can be controlled, the performance of SWCNT is highly improved. On the other hand, the entangled structure of SWCNTs have merits for application to fabricated films which are requested as flat panels and for separation technologies. Therefore, control of the bundle structures of SWCNTs is indispensable to extend their application field.

However, it is not so easy to dissociate the bundle structure and refabricate the entangled structure, although the inter-tube interaction stems from van der Waals attractive interaction. Many researchers have tried to disperse the

SWCNT bundles with surfactants, surface functionalization, organic solvents, or acids with the aid of ultrasonication (Moore et al. 2003; Paredes and Bueghard 2004; Tan and Resasco 2005; Yang et al. 2005).

It has been reported that high power ultrasonication treatment is efficient to disperse the SWCNT bundles in an oxidative solution (Komiyama et al. 2005; Zhang et al. 2003; Ziegler et al. 2005). Nevertheless, the nanopore structural change of the entangled SWCNT bundles after the sonication treatment was not clearly elucidated. In the present study, the nanopore structural change of SWCNT bundles with ultrasonicated treatment in H_2O_2 solution was clarified with careful analysis of high resolution N_2 adsorption isotherms in addition to Raman spectroscopic and electron microscopic examination.

2 Experimental

SWCNT samples, which are so-called HiPco SWCNTs, were prepared by the high pressure carbon monoxide process using Fe catalysts (Carbon Nanotechnologies Inc.). Thermal gravimetric analysis of SWCNT was carried out in an O_2 atmosphere up to 1473 K (SII EXSTAR6000); the amount of Fe catalyst was 11 wt%. SWCNT samples weighing 10 mg were immersed in 100 ml of 5% H_2O_2 solution, which sonicated in an ice bath under the sonication conditions of 750 W and 20 kHz for different times of 1 to 12 h using (Sonica & Materials, Inc. Ultrasonic processor VC-750). The ultrasonic wave was irradiated with every 1 second. The resultant SWCNT-H_2O_2 suspensions were filtrated and then dried at ambient temperature for a few days. The ultrasonication-treated SWCNTs were characterized with scanning electron microscopy (JEOL JSM-6330), high resolution transmission microscopy (JEOL JEM-4000FXII), Raman spectroscopy (JASCO NRS-3100), and high resolution N_2 adsorption method. The N_2 adsorption isotherm of the treated SWCNT was measured at 77 K after the pre-evacuation at 473 K for 2 h using a volumetric system (Quantachrome Instruments Autosorb-1 Series). The N_2 adsorption isotherm was analyzed with grand canonical Monte Carlo (GCMC) simulation.

3 GCMC simulation

The established GCMC simulation method gave the adsorption isotherms of N_2 at 77 K on SWCNT which diameter is 1.36 nm (Suzuki et al. 1996; Ohba and Kaneko 2002; Tanaka et al. 2005; Cheng et al. 2004; Gu et al. 2001; Simonyan et al. 1999). The random movement, creation, and removal of molecules make new configurations. They are accepted when they obey Metropolis's sampling scheme in proportion to $\exp(-\Delta E/kT)$ where ΔE is the change of total energy in the system. Each step of the scheme in GCMC simulation was calculated 10^7 cycles.

Lennard-Jones (LJ) potential is adopted to model C-C, C-N_2 and N_2-N_2 interactions. LJ potential is given by

$$\Phi(r) = 4\varepsilon_{ij}\left\{\left(\frac{\sigma_{ij}}{r}\right)^{12} - \left(\frac{\sigma_{ij}}{r}\right)^{6}\right\}$$

where r denotes the distance between the center of particle i and particle j and Φ denotes the potential energy. In actual calculation, $\sigma_{NN} = 3.32$ nm, $\varepsilon_{NN}/k_B = 36.4$ K, $\sigma_{CN} = 3.36$ nm, and $\varepsilon_{CN}/k_B = 33.4$ K were used. Here [NN] and [CN] indicate N_2-N_2 and carbon atom-N_2 pair interactions, respectively.

4 Results and discussion

4.1 Morphological structure change

Figure 1 shows SEM images of SWCNTs ultrasonicated for different time. The bundles of the SWCNTs are entangled each other in the SEM image of raw SWCNT. The bundle ropes become finer with the ultrasonicated time up to 3 h. We can observe many fine bundles whose diameter is less than 20 nm due to untangling. On the contrary the ultrasonication treatment for 6 h leads to bolder ropes of ∼500 nm in diameter. The 12 h-ultrasonication treatment shortens the bold rope length. The ultrasonications for more than 6 h partially cut and dissociate the SWCNT bundles to provide densely entangled structures. Thus, the ultrasonication treatment of SWCNTs in H_2O_2 solution is quite effective to change the bundle and entangled structures. High resolution TEM observation gives more definite information, as shown in Fig. 2. We often observe the bundle structure, which consists of several SWCNTs, with less than 10 nm in diameter on the TEM image of the SWCNT sample treated for 1 h. The TEM image of the SWCNTs treated over 6 h showed that many SWCNTs are broken, producing amorphous carbons. The defective structural change was examined with Raman spectroscopy. Figure 3 shows D and G bands of SWCNT as a function of the sonication treatment time. The basic SWCNT structure is preserved even after the 12 h-treatment, because the G-band is predominant compared with the D-band. The ultrasonication treatment decreases the G/D band intensity ratio; the G/D band intensity ratio vs. ultrasonication treating time of the treated samples has a maximum at 3 h. As the G/D band intensity ratio is directly associated with the defective structure of SWCNT samples, the ultrasonication treatment for 3 h can dissociate efficiently the bundles without great structure damages, which agrees with the SEM and TEM observations. The G-band consists of the G^+ band at 1600 cm^{-1} and G^- band at 1550 cm^{-1}. G^+ and G^- bands originate from atomic displacement along the tube axis and circumferential direction, respectively. The G-band varies dramatically due to the

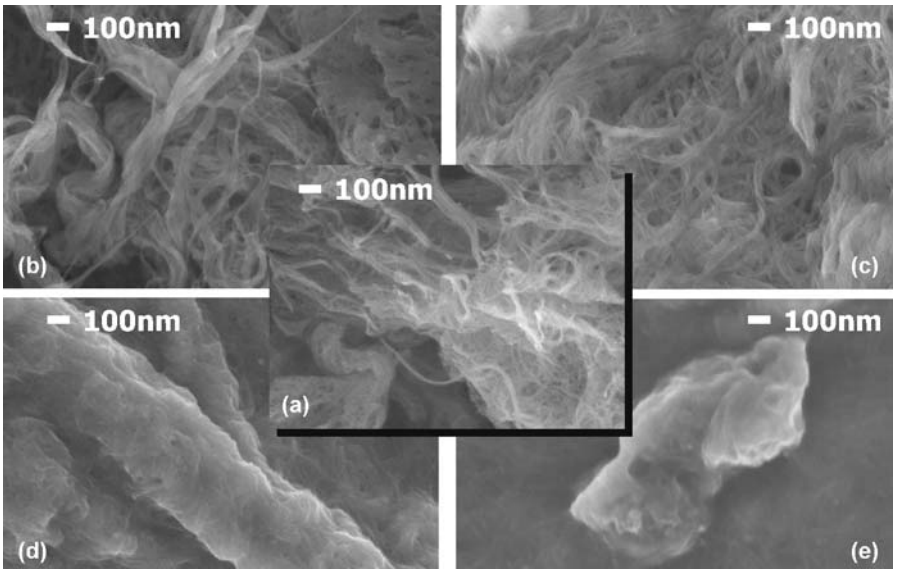

Fig. 1 SEM images of SWCNTs sonicated for different time. (**a**) Raw SWCNT, (**b**) 1 h, (**c**) 3 h, (**d**) 6 h, and (**e**) 12 h

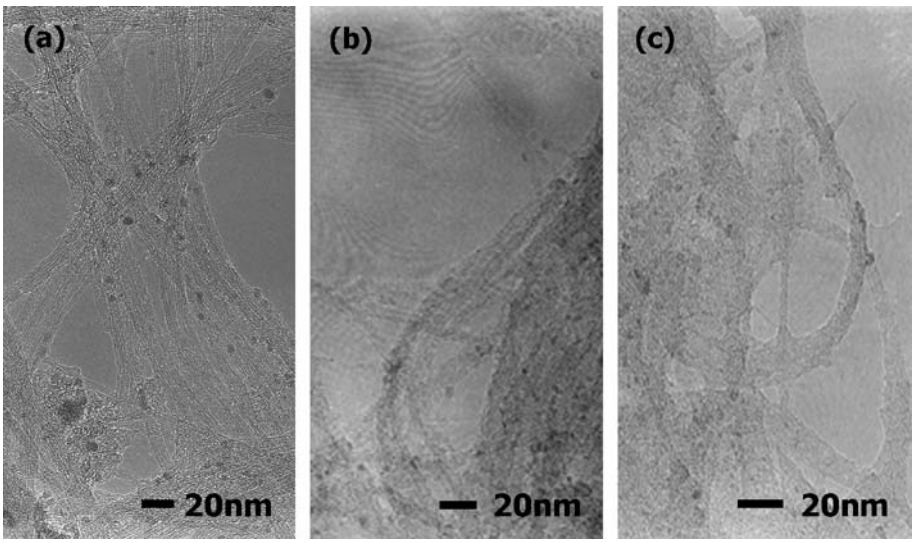

Fig. 2 TEM images of SWCNTs sonicated for different time. (**a**) Raw SWCNT, (**b**) 1 h, and (**c**) 12 h

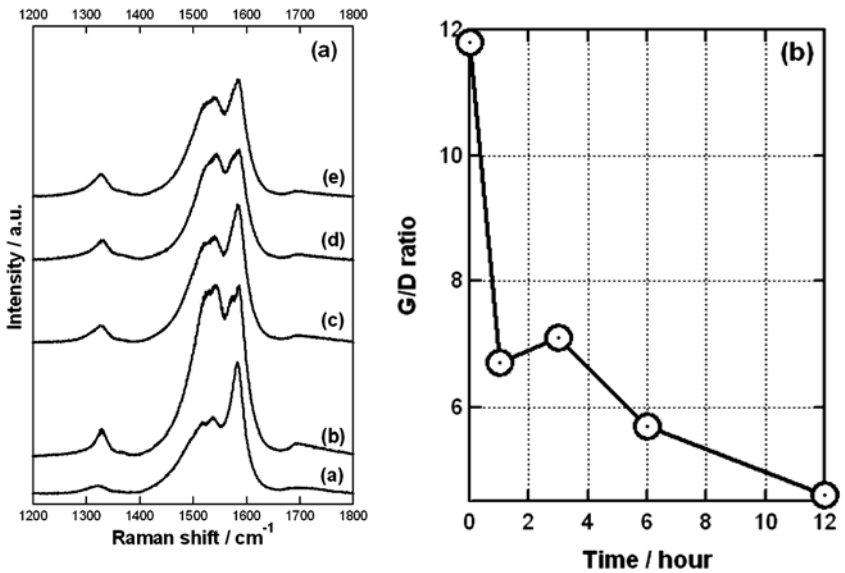

Fig. 3 (**a**) Raman spectra (D, G-band) of sonicated samples. ((*a*) Raw SWCNT, (*b*) 1 h, (*c*) 3 h, (*d*) 6 h, and (*e*) 12 h), and (**b**) G/D ratio vs. sonication time

treatment; the intensity of the G^+ band decreases to become comparable to that of the G^- band after the treatment, as shown in Fig. 3. Consequently, long sonication treatment collapses partially the SWCNT structure to shorten the tube length. At the same time, semiconductive SWCNTs should be decomposed through the longer treatment (Jorio et al. 2003) and then relatively metallic SWCNTs increases, giving a stronger G^- band. On the other hand, the RBM bands do not change, as shown in Fig. 4. The sonication treatment does not change the distribution of the tube diameter (Kataura et al. 1999). Accordingly, the formation of the bold aggregation due to the sonication for more than 6 h should come from the firm assembly formation of tubes cut by the ultrasonication in H_2O_2 solution.

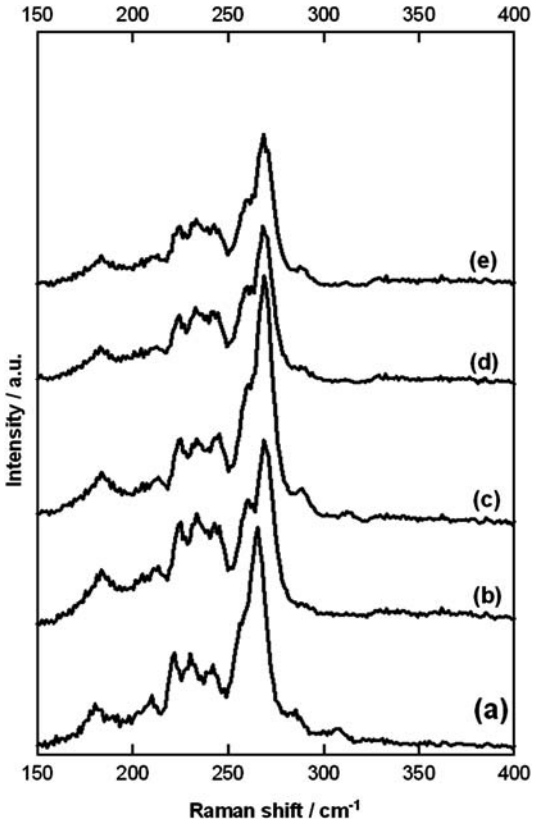

Fig. 4 Raman spectra (RBM) of sonicated samples. (*a*) Raw SWCNT, (*b*) 1 h, (*c*) 3 h, (*d*) 6 h, and (*e*) 12 h

4.2 Nanopore structural change

Figure 5a shows N_2 adsorption isotherms of SWCNTs treated for different durations. The N_2 adsorption amount increases with the treating time up to 3 h, and then remarkably decreases due to the further treatment. The N_2 adsorption isotherms whose abscissa is expressed in terms of logarithm of P/P_0 are also shown in Fig. 5b. The N_2 adsorption isotherms of SWCNT samples treated for 1 and 3 h are of IUPAC Type II, whereas N_2 adsorption isotherms of both samples treated for 6 and 12 h are close to IUPAC Type I. The Type II adsorption isotherm is observed for the adsor-

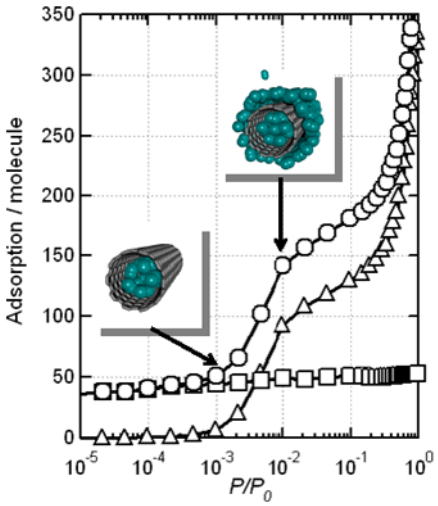

Fig. 6 GCMC simulated N_2 adsorption isotherm of single SWCNT at 77 K together with snapshots. ○: Total, □: in internal space, and △: on external space

Fig. 5 N_2 adsorption isotherms of SWCNTs treated for different times, at 77 K (**a**), logarithm relative pressure (**b**). ○: Raw SWCNT, ●: 1 h, □: 3 h, ■: 6 h, and △: 12 h

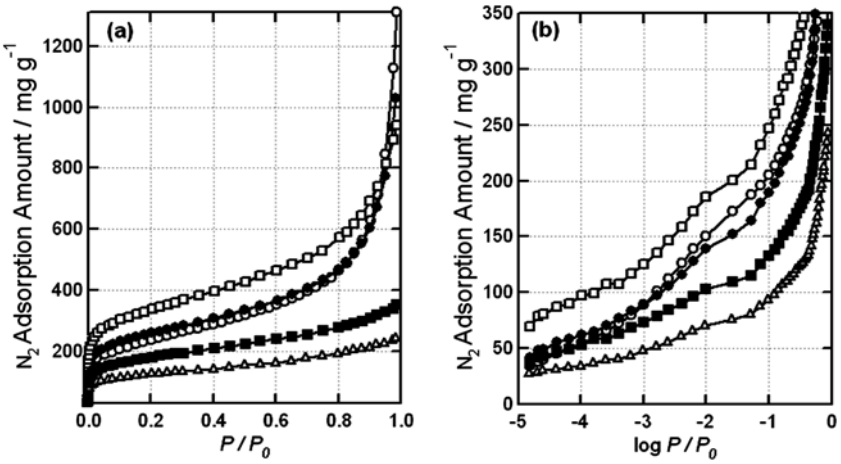

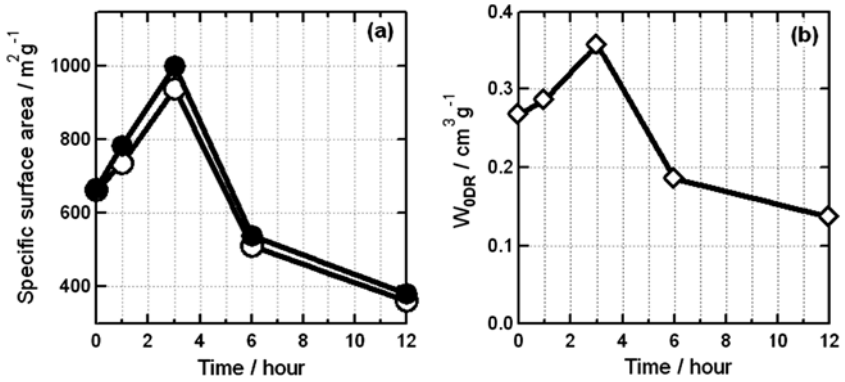

Fig. 7 Variation of specific surface area (**a**) and micropore volume (**b**). ○: BET, ●: SPE method

bent whose external surface area is predominant compared with the pore surface area. On the contrary, the presence of sufficient amount of micropores leads to Type I. Accordingly, the sonication treatment for 3 h dissociates the bundle structure to very fine ones, giving a greater adsorption amount in the whole P/P_0 region. The treatment for more than 6 h induces the aggregation of bundles whose external surfaces become nil, compared with the micropore surfaces. At the same time, even micropores should be partially blocked by amorphous carbons by the treatment, providing the Type I isotherm. These results coincide with the morphological changes. A better information on adsorption in micropores is provided from Fig. 5b, because adsorption in micropores begins even below $P/P_0 = 10^{-3}$. We can observe a gradual step around $P/P_0 = 10^{-3} \sim 10^{-2}$. Figure 6 shows the GCMC simulated N_2 adsorption isotherm of single SWCNT at 77 K together with snapshots. This simulated isotherm explicitly indicates that adsorption in the internal pore space finishes below $P/P_0 = 10^{-3}$. Therefore, adsorption below $P/P_0 = 10^{-3}$ should stem from filling in the internal pore spaces. As real SWCNT samples have the bundle structure, adsorption above $P/P_0 = 10^{-3} \sim 10^{-2}$ should be a combined process of adsorption in interstitial pores and on the external surfaces of the bundle.

The N_2 adsorption isotherms were analyzed with the BET, α_s, and DR plots, providing the surface area, micropore volume, and isosteric heat of adsorption at the fractional filling of e^{-1}. Figure 7 shows changes of surface area and micropore volume with the ultrasonic treatment time. The BET surface area is slightly smaller than the surface area from the subtracting pore effect (SPE) method with α_s-plot. The SPE method using the α_s-plot gives a more correct surface area than the BET surface area (Setoyama et al. 1998). Both surface area vs. treating time plots are very similar. The surface area increases until 3 h, accompanying with a remarkable drop. The surface area is associated with the bundle size after Williams et al.; the SWCNT bundle after 3 h should consist of six SWCNTs and the further ultrasonication should enlarge the bundle of about fifty SWCNTs (Williams and Eklund 2000; Agnihotsi et al. 2005). The bundle size of the SWCNT after the 6 h-treatment from N_2 adsorption is larger than that by the SEM and TEM observation. The discrepancy should come from blocking of micropores with amorphous carbon particles. In order to remove the blocking effect, we subtracted the amount adsorbed in internal and interstitial pores, which can be approximated by the adsorption amount at $P/P_0 = 10^{-3}$, referring the GCMC results. The average tube diameters of about 1 nm determined from the RBM bands was for the surface area evaluation. Thus-obtained relationship between the surface area and tube number indicates that average tube number decreases up to 8 by the sonication for 3 h and increases up to 40 by the sonication 12 h. The micropore volume change is almost similar to the surface area change, as shown in Fig. 7b.

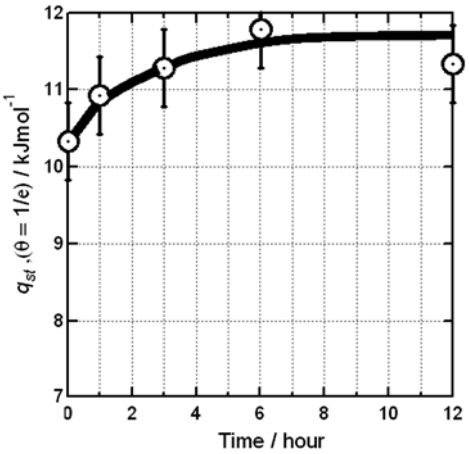

Fig. 8 The isosteric heat of $q_{st}, \theta = e^{-1}$ adsorption change of SWCNT samples with the treating time

Figure 8 shows the $q_{st}, \theta = e^{-1}$ increases until 6 h and becomes almost constant after 6 h; the $q_{st}, \theta = e^{-1}$ is in the range of 10.3–11.7 kJ mol^{-1}, being not so different from that observed in the slit pores of ACF (11 kJ mol^{-1}) (Kaneko et al. 1989). The difference between these $q_{st}, \theta = e^{-1}$ values is within 2 kJ mol^{-1}. The bold SWCNTs should be selectively collapsed during the ultrasonic treatment, giving a little larger $q_{st}, \theta = e^{-1}$ value for the treated sample for a

longer time. Also less contribution of adsorption on the external surfaces for the treated SWCNT samples for a longer time must increase the $q_{st}, \theta = e^{-1}$ value slightly.

Thus, an optimum ultrasonic treatment in H_2O_2 solution can shorten SWCNTs, dissociating the bundle structure. Hence, this treatment can be applied to produce SWCNT sheet having a great microporosity.

Acknowledgement This work was supported by Grant-in-Aids for Scientific Research (S) (No. 15101003) by JSPS.

References

Agnihotsi, S., Mota, J.P.B., Rosta-Abadi, M., Rood, M.J.: Structural characterization of single-walled carbon nanotube bundles by experimental and molecular simulation. Langmuir **21**, 896–904 (2005)

Cao, D., Zhang, X., Chen, J., Wang, W., Yun, J.: Optimization of single-walled carbon nanotube arrays for methane storage at room temperature. J. Phys. Chem. B **107**, 13286–13292 (2003)

Cheng, J., Yuan, X., Zhao, L., Huang, D., Zhao, M., Dai, L., Ding, R.: GCMC simulation of hydrogen physisorption on carbon nanotubes and nanotube arrays. Carbon **42**, 2019–2024 (2004)

Gu, C., Gao, G., Yu, Y., Mao, Z.: Simulation study of hydrogen storage in single walled carbon nanotubes. Hydrogen Energy **26**, 691–696 (2001)

Hata, K., Futaba, D.N., Mizuno, K., Namai, T., Yumura, M., Iijima, S.: Water-assisted highly efficient synthesis of impurity-free single-wall carbon nanotubes. Science **306**, 1362–1364 (2004)

Hirsch, A.: Functionalization of single-walled carbon nanotubes. Angew. Chem. Int. Ed. **41**, 1853–1859 (2002)

Jorio, A., Dimenta, M.A., Filho, A.G.S., Saito, R., Dresselhaus, G., Dresselhaus, M.S.: Characterizing carbon nanotube samples with resonance Raman scattering. New J. Phys. **5**, 139.1–139.17 (2003)

Kaneko, K., Fukuzaki, N., Kakei, K., Suzuki, T., Ozeki, S.: Enhancement of NO dimerization by micropore fields of activated carbon fibers. Langmuir **5**, 960–966 (1989)

Kataura, H., Kumazawa, Y., Maniwa, Y., Umezu, I., Suzuki, S., Ohtsuka, Y., Achiba, Y.: Optical properties of single-wall carbon nanotubes. Synth. Met. **103**, 2555–2558 (1999)

Komiyama, S., Miyawaki, H., Okino, F., Kataura, H., Touhara, H.: Structure of nanocarbons and their lithium ion secondly battery anode properties. TANSO, 25–33 (2005)

Moore, C., Strano, M.S., Haroz, E.H., Hauge, R.H., Smalley, R.E.: Individually suspended single-walled carbon nanotubes in various surfactants. Nano Lett. **3**, 1379–1382 (2003)

Ohba, T., Kaneko, K.: Internal surface area evaluation of carbon nanotube with GCMC simulation-assisted N_2 adsorption. J. Phys. Chem. B **106**, 7171–7176 (2002)

Paredes, J.I., Bueghard, M.: Dispersion of individual single-walled carbon nanotubes of high length. Langmuir **20**, 5149–5152 (2004)

Saito, R., Dresselhaus, G., Dresselhaus, M.S.: Trigonal warping effect of carbon nanotubes. Phys. Rev. B **61**, 2981–2990 (2000)

Setoyama, N., Suzuki, T., Kaneko, K.: Simulation study on the relation ship between a high resolution α_s-plot and the pore size distribution for actuated carbon. Carbon **36**, 1459–1467 (1998)

Simonyan, V.V., Diep, P., Johnson, J.K.: Molecular simulation of hydrogen adsorption in changed single-walled carbon nanotubes. J. Chem. Phys. **111**, 9778–9783 (1999)

Suzuki, T., Kaneko, K., Setoyama, N., Maddox, M., Gubbins, K.E.: Grand canonical Monte Carlo simulation for nitrogen in graphitic slit micropores: effect of interlayer distance. Carbon **34**, 909–912 (1996)

Tan, Y., Resasco, D.E.: Dispersion of single-walled carbon nanotubes of narrow diameter distribution. J. Phys. Chem. B **109**, 14454–14460 (2005)

Tanaka, H., Fan, J., Kanoh, H., Yudasaka, M., Iijima, S., Kaneko, K.: Quantum nature of adsorbed hydrogen on single-wall carbon nanohorns. Mol. Simul. **31**, 465–474 (2005)

Williams, K.A., Eklund, P.C.: Monte Carlo simulation of H_2 physisorption in finite-diameter carbon nanotubes ropes. Chem. Phys. Lett. **320**, 352–358 (2000)

Yang, C., Park, J.S., An, K.H., Lim, S.C., Seo, K., Kim, B., Park, K.A., Han, S., Park, C.Y., Lee, Y.H.: Selective removal of metallic single-walled carbon nanotubes with small diameters by using nitric and sulfuric acid. J. Phys. Chem. B **109**, 19242–19248 (2005)

Zhang, J., Zou, H., Qing, Q., Yang, Y., Li, Q., Liu, Z., Guo, X., Du, Z.: Effect of chemical oxidation on the structure of single-walled carbon nanotubes. J. Phys. Chem. B **107**, 3712–3718 (2003)

Ziegler, K.J., Gu, Z., Peng, H., Flor, E.L., Haouge, R.H., Smalley, R.E.: Controlled oxidative cutting of single-walled carbon nanotubes. J. Am. Chem. Soc. **127**, 1541–1547 (2005)